A Novel Modified Space Vector Pulse Width Modulator Based on Artificial Neural Network for Z-Source Inverter

Dr. Majid K. Al-khatat
Electrical Engineering Department, University of Technology/Baghdad
Lina J. Rashad
Electrical Engineering Department, University of Technology/Baghdad
Email: lina.j.rashad@gmail

Received on:10/9/2015 & Accepted on:21/4/2016

ABSTRACT

This paper proposes a novel modified space vector pulse width modulator based on Artificial Neural Network (ANN). This method overcomes the drawbacks of conventional DSP-based modulator in the z-source inverter. This generates timing signals without computations delay time, which increases the capability of using high switching frequency. Moreover, the proposed method overcomes the nonlinearity relationship between modulation index and the boosting factor during buck and boost regions. The simulation of the proposed system is fully evaluated for different operation condition. The schemes and training of the proposed neural networks are presented and examined with respect to conventional DSP-based method. Simulation results show excellent performance for both AC-side and DC-side of the Z-source inverter for different output voltages. In addition, the proposed ANN-based modulator operates very well in both buck and boost mode and overcomes the discontinuity of modulation index and the boosting factor. The voltage stress across the devices in the proposed method is less than of the conventional DSP-based method especially for high gain operation condition.
Keywords: Z-source inverter modified SVPWM, ANN.

INTRODUCTION

The output voltage obtained by a traditional voltage source inverter can never exceed the DC-link voltage. Thus it considered as buck-converter. If a higher output voltage is required, an additional DC-DC boosting stage can cascaded to the voltage-source inverter, which increase the complexity and reduce the reliability of the inverter. In the conventional Voltage Source Inverter (VSI) the two switches of the same-phase leg can never be gated-on at the same line because doing so cause a short circuit (shoot-through) to occur, which would destroy the inverter. Thus a dead time is inserted between transition-states to avoid short circuit state; this may distort the output voltage. These limitations of the traditional voltage source inverter can overcome by using the Z-source inverter [1]. Fig. 1 shows the general Z-source inverter structure. The impedance-source inverter employs a unique impedance network which is consists of two inductors L_1 and L_2 and capacitors C_1 and C_2 connected as X shape to link between the inverter circuit and the DC power supply [2].

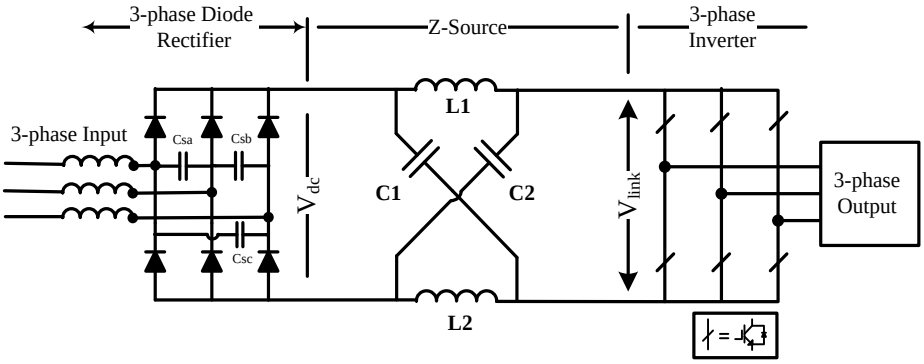

Figure(1). General structure of ZSI

Unlike the traditional voltage-source inverter that has eight states, the three phase bridge ZSI has nine permissible switching states. The VSI has six active vectors and two zero vectors. However, the three phase bridge ZSI has one additional zero state when the two devices of any leg are gated on. This third zero state is called the shoot-through zero state, which can be generated by seven different ways: shoot-through via any one legs, combinations of any two phases legs and all three-phase legs. This shoot-through zero state provides the unique buck-boost feature to the inverter [3, 5]. The overall voltage gain of the ZSI system (G) depends on two factors: the traditional modulation index (M) and the boosting factor (B) where G=MB and B=1/ (1-2D_{sh}), where D_{sh} is the shoot-through duty ratio. By selecting suitable values of the shoot-through duty ratio and modulation index, both of DC-link and output AC voltage can be controlled to the desired values. The selection of proper value of the shoot-through duty ratio is very important matter to avoid excessive voltage stress across the inverter devices, which may reduce their life and may increase cost. The relationship between the voltage gain and both of the modulation index and the shoot-through duty ratio is highly nonlinear variation over the buck and boost operation modes. Therefore, there are many methods for controlling the impedance network used the carrier-based methods such as: simple boosting control method, maximum boosting control method [6], and maximum constant boosting control method [7]. Fig. 2 shows the relationship between the M, D_{sh} and G.

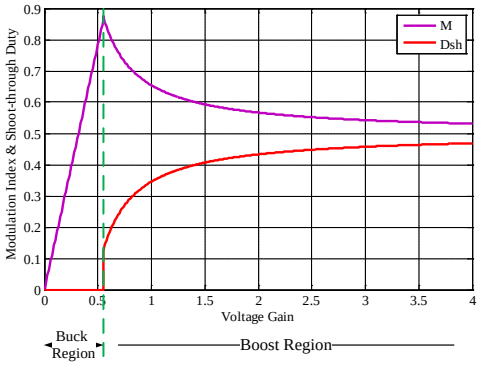

Figure(2). Relationship between M, D_{sh} and G

SVPWM techniques have been developed in recent investigations, which called a modified space vector pulse width modulation MSVPWM, since these techniques are more favorable to control the shoot-through duty ratio in the Z-network [8]. The MSVPWM pattern gives a wide operating region for a desired AC output voltage and reduces the voltage stress across devices. However, complex online computation that usually limits its operation up to several kilo hertz of switching frequency is the disadvantage of MSVPWM. Switching frequency can be expanded by using a DSP (high-speed digital processor) and simplicity computations with help of lookup tables. Since lookup tables are very large, it leads to reduce the pulse width resolution [9]. So the high speed digital processor-based MSVPWM practically cannot use in this region while ANN-based MSVPWM can possibly take over.

Nowadays, the application of artificial neural networks is recently increased in power electronic systems. A feed foreword artificial neural network implements nonlinearity input-output mapping. The computational delay of this mapping can neglect if parallel architecture of the network can be carried out by an application specific integrated circuit (ASIC) chip.

This paper proposed feed foreword ANN-based MSVPWM that fully covers the back and boost regions by calculation the proper timing sequenceT_o, T_1, T_2 and T_{sh} (which will be defined in detail in the next section) for each desired AC output voltage. Moreover, this paper proposed a separately ANN to calculate the proper value of the modulation index and the shoot-through duty ratio for the desired output DC voltage in order to reduce the voltage stress across the devices. A back propagation type feed foreword ANN is trained offline with the data generated by this simple algorithm, and the extensively evaluated on buck-boost operation of the impedance-source inverter.

Operation principle:

The impedance-source inverter can produce any desired AC output voltage from any DC input voltage. However, the three-phase ZSI has one additional zero vector besides the six active voltage vectors and two zero vectors in the conventional VSI and Current Source Inverter (CSI).

The ZSI has three operation modes which are called: normal mode, zero state mode, and shoot-through mode. In normal mode and zero state modes, the ZSI operates like the conventional PWM inverter. In the shoot-through mode, the load terminals are shorted both the upper and lower switching devices of any phase legs. The DC capacitor voltage (V_C) can be increased to the desired value, and the shoot-through state is neglected in the conventional inverters. The capacitor voltage equation is given [10]:

$$V_C = \frac{T_S - T_{sh}}{T_S - 2T_{sh}} V_{dc} = \frac{1 - D_{sh}}{1 - 2D_{sh}} V_{dc} \quad \text{... (1)}$$

Where, $D_{sh} = \frac{T_{sh}}{T_S}$ is the shoot-through duty ratio forT_{sh}.

The stress voltage of the switching devices (V_{Link}) is given:

$$V_{Link} = \frac{1}{T_S - 2T_{sh}} V_{dc} = \frac{1}{1 - 2D_{sh}} V_{dc} \quad \text{… (2)}$$

The ratio between the V_C and V_{Link} with DC input voltage versus D_{sh} are mapped in fig. 3. When D_{sh} increases from 0 to 0.5, the V_C is boosted and the V_{Link} is greater than the V_C. As D_{sh} approached 0.5, both the capacitor voltage and stress voltage increase to infinite. The unique feature of Z-source inverter is that The V_C can be increased more times than the DC input voltage by controlling the shoot-through time (T_{sh}) without extra DC boost converter.

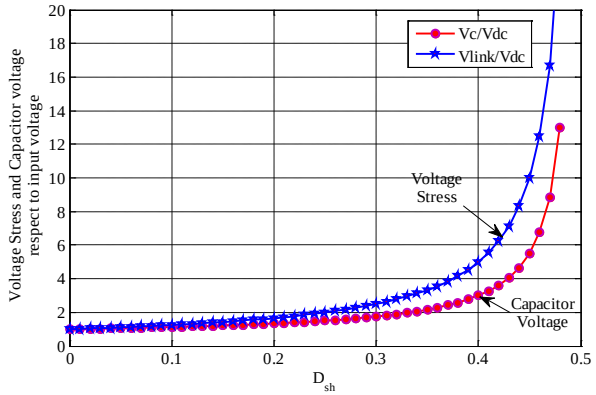

Figure(3). Voltage stress and capacitor voltage with respect to D_{sh}

Modified Space Vector PWM (MSVPWM):

The space vector pulse width modulation is more suitable to control the T_{sh} in the Z-source inverter. The eight space vectors V_0-V_7 illustrated in fig. 4, are used in conventional SVPWM, where V_1-V_6 are active vectors, and V_0 and V_7 are null vectors. If the reference voltage vector V_{ref} is located between the arbitrary vector V_1 and V_2, the reference voltage vector divided into two adjacent voltage vectors (V_k and V_{k+1}) and null vectors (V_0 and V_7).

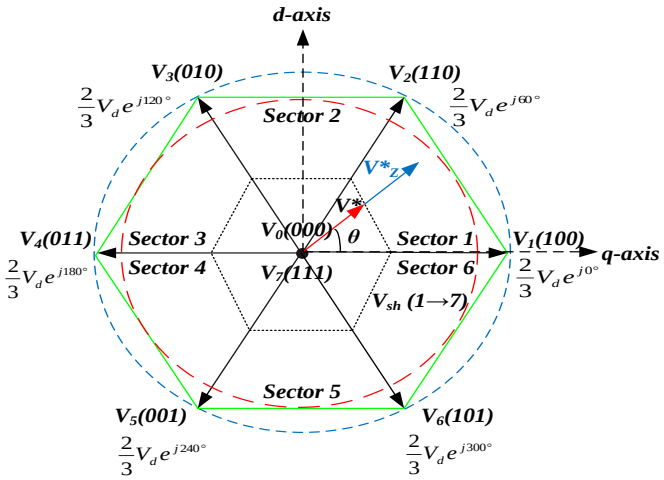

Figure(4). Voltage trajectory of the space vectors

In a sampling inverter T_s, voltage vectors V_k and V_{k+1} are applied during T_1 and T_2, respectively, and the null vectors are applied during T_o=T_s-(T_1+T_2). The reference voltage vector V_{ref} is written as follows [11].

$$\vec{V}_{ref} = T_1\vec{V}_k + T_2\vec{V}_{k+1} + T_o(\vec{V}_0 \; or \; \vec{V}_7) \quad \ldots (3)$$

The time interval can be obtained as [12]:

$$T_1 = \sqrt{3}\,\frac{|\vec{V}_{ref}|}{\vec{V}_k} T_S \sin(n\frac{\pi}{3} - \theta) \quad \ldots(4)$$

$$T_2 = \sqrt{3}\,\frac{|\vec{V}_{ref}|}{\vec{V}_k} T_S \sin(\theta - \frac{(n-1)}{3}\pi) \quad \ldots(5)$$

Where

θ is the angle between the V_{ref} and V_1, and n is the number of sector in which reference vector is located.

The symmetrical switching pattern of voltage vectors V_1 , V_2 and zero vectors V_0 and V_7 during one sampling period at the MSVPWM is illustrated in fig. 5. Unlike the conventional space vector PWM, the MSVPWM has an extra shoot-through period T_{sh} besides active state time intervals T_1 , T_2 and T_o . The zero voltage period must be modified for generating the shoot-through time interval is evenly assigned to each phase with $T_{sh}/3$, which the time intervals T_1 and T_2 are not change.

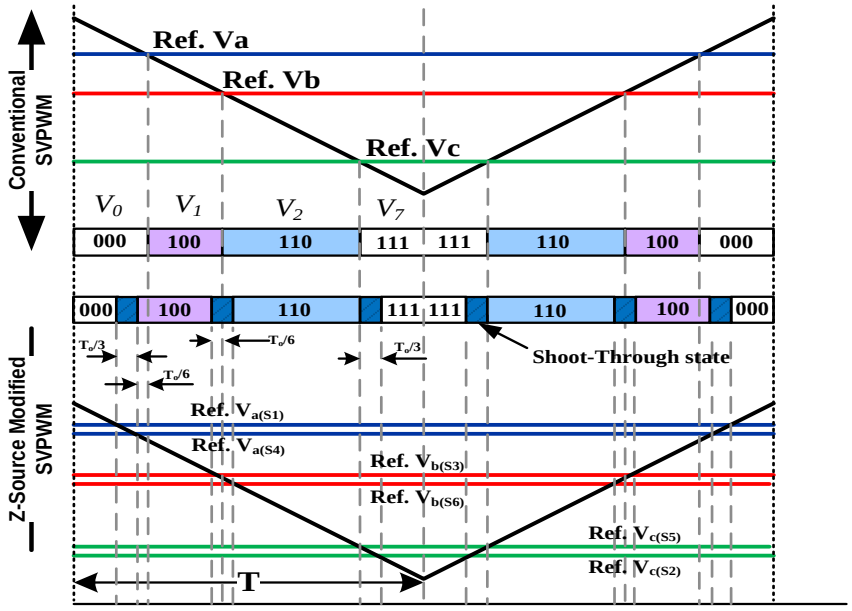

Figure(5). The conventional and MSVPWM Switching pattern

Voltage stress limitation:

The second zero vector time interval V_7, as seen in fig. 5, is equal to ($T_o/4$-$T_{sh}/3$). It's essentially to maintain this interval greater than zero and positive, therefore the shoot-through time is limited to $3T_o/4$:

$T_{sh} = \frac{3}{4}T_o \rightarrow \frac{T_{sh}}{T_s} = \frac{3}{4}\frac{T_o}{T_s} = \frac{3}{4}\left(\frac{T_s-(T_1+T_2)}{T_s}\right) = \frac{3}{4}\left(1 - \frac{(T_1+T_2)}{T_s}\right)$ … (6)

The active state time interval T_a in sector-1 can be determined from equations (4) and (5):

$n = 1 \rightarrow T_a = T_1 + T_2 = \sqrt{3}\ \frac{|\vec{V}_{ref}|}{\vec{V}_k} T_s \sin(\theta + \frac{\pi}{3})$ …(7)

Since the angle of each sector is $\pi/3$, therefore the active time interval T_a varies periodically during any $\pi/3$ interval. Therefore the average of T_a can be determined between 0 and $\pi/3$ [13].

$(T_a)_{avg} = \frac{1}{(\pi/3)}\int_0^{\pi/3} \sqrt{3}\ \frac{|\vec{V}_{ref}|}{\vec{V}_k} T_s \sin(\theta + \frac{\pi}{3})\, d\theta$ . ...(8)

Since $\vec{V}_{ref} = \hat{V}_{ac}$. Where: $\hat{V}_{ac}$ is the magnitude of the ac output voltage, then:

$(T_a)_{avg} = \frac{3\sqrt{3}}{\pi} T_s \frac{\hat{V}_{ac}}{\hat{V}_k} = \frac{3\sqrt{3}}{2\pi} T_s \frac{\hat{V}_{ac}}{\hat{V}_k/2}$ …(9)

And then:

Since $\frac{\hat{V}_{ac}}{\hat{V}_k/2} = \text{modulation index } (M) \rightarrow (T_a)_{avg} = \frac{3\sqrt{3}\ M}{2\pi} T_s$

$\rightarrow \frac{T_{sh}}{T_s} = \frac{3}{4}\left(1 - \frac{(T_a)_{avg}}{T_s}\right) = \frac{3}{4}\left(1 - \frac{3\sqrt{3}\ M}{2\pi}\right)$

$\rightarrow \frac{T_{sh}}{T_s} = \frac{3}{4}\left(\frac{2\pi - 3\sqrt{3}\ M}{2\pi}\right)$ …(10)

$\therefore \text{Boost factor } (B) = \frac{1}{1-(2T_{sh}/T_s)} = \frac{4\pi}{9\sqrt{3}\ M - 2\pi}$

(11)

$\therefore \text{Shoot} - \text{through duty ratio } (D_{sh}) = \frac{3}{4}.\frac{2\pi - 3\sqrt{3}\ M}{2\pi}$ … (12)

$\therefore \text{Voltage gain } (G) = MB = \frac{\hat{V}_{ac}}{\hat{V}_{dc}/2} = \frac{4\pi M}{9\sqrt{3}\ M - 2\pi}$ …(13)

Also for given voltage gain, the modulation index is:

$M = \frac{2\pi G}{9\sqrt{3}\ G - 4\pi}$ … (14)

1. Modified Reference (MR) for controlling ZSI:

MR modulation of three-phase Z-source inverter is shown in fig. 5 where six modified references are used for controlling the six inverter switches independently [14]. Mathematically, the modified references are expressed as:

$$\left.\begin{aligned} V_{max}(s\ upper) &= V_{max} + V_{off} + T_1 \\ V_{max}(s\ lower) &= V_{max} + V_{off} + T_2 \\ V_{mid}(s\ upper) &= V_{mid} + V_{off} + T_2 \\ V_{max}(s\ lower) &= V_{mid} + V_{off} - T_2 \end{aligned}\right\}$$

(15)

$$\left.\begin{aligned} V_{min}(s\ upper) &= V_{min} + V_{off} - T_2 \\ V_{min}(s\ lower) &= V_{min} + V_{off} - T_1 \end{aligned}\right\}$$

$T_1 = {}^{T_{sh}}/_{T};\ T_2 = {}^{T_{sh}}/_{3T}$

Where $V_{max} = max(V_a, V_b, V_c)$, $V_{mid} = mid(V_a, V_b, V_c)$, $V_{min} = min(V_a, V_b, V_c)$ are three sinusoidal references and V_{off} is the triple offset needed for implementing alternative PWM with different null state placements. For this work, the offset of $V_{off} =$

$-0.5(V_{max}+V_{min})$ is used to maintain equal null durations at the start and end of a half carrier period to achieve optimal harmonic performance [14]. Using equation 15 and the chosen offset typical modified references for phase-A is shown in fig. 6.

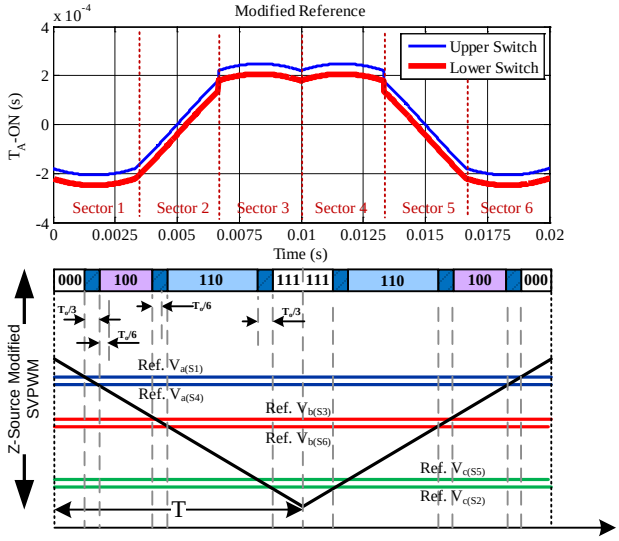

Figure(6). Modified reference signal for MSVPWM

Where three shoot-through states are inserted immediately adjacent to the active states with the active intervals kept constant to maintain the correct volt-sec average. Specifically, $V_{max}(s\ upper)=V_a(S_1)$ and $V_{max}(s\ lower)=V_a(S_4)$ in fig. 6 are for inserting the first shoot-through state by turning ON S_1 and S_4, $V_{mid}(s\ upper)=V_b(S_3)$ and $V_{mid}(s\ lower)=V_b(S_6)$ are for second shoot-through state by turning ON S_3 and S_6 , and $V_{min}(s\ upper)=V_c(S_5)$ and $V_{min}(s\ lower)=V_c(S_2)$ are for the last shoot-through state by turning ON S_5 and S_2. Instead of three shoot-through states, a modification to equation 15 can be done by changing T_1 and T_2 to $T_{sh}/_{2T}$ and 0 respectively for inserting any two shoot-through states within the null intervals at the start and end of a half carrier cycle.

ANN-based modified SV modulator:

As mentioned earlier, MSVPWM is one of the best modulation methods in digital applications. Although, in principle, it is an easy task to implement MSVPWM in digital system, however, required computational efforts and corresponding time needed to run the programs limit maximum sampling frequency and bandwidth of the control system.

In real-time implementation of MSVPWM, first, position and magnitude of each reference vector should be determined in a complex plane for each switching cycle (sector number, $|V_{ref}|$ and θ), and then modulation method, these functions are stored in a table kept in the necessary and interpolation is used to determine their approximate values based on the position and magnitude of the reference voltage vector in the complex plane and for each sampling instant. This method has three drawbacks: (i) it

needs a large memory and this increases the hardware requirements. (ii) Imprecision caused by the interpolation of non-linear functions results in distortion in harmonic spectrum of PWM waveforms. (iii) Interpolation increases computational time and effort, thereby limiting maximum sampling frequency of the inverter. Moreover, as illustrated before, the selection of the proper value of the modulation index (M_i) and the shoot-through duty ratio (D_{sh}) is somewhat difficult for the purpose of reduce the voltage stress across the devices. The method proposed in this paper uses ANNs to overcome these drawbacks.

The derivation of turn-on time $T_A - ON$ for the upper and lower switches and the determination of the optimal value of modulation index and the shoot-through duty ratio permit ANN-based MSVPWM implementation using two separate subnets: first is the modulation index and shoot-through duty ratio subnet which uses a multilayer perception type network with sigmoid type transfer function. The composite network uses two input neurons, four neurons in the hidden layer, and two output neurons. The input signals are the desired AC output voltage $|\hat{V}_{ph}|$ and the available DC supply (V_{dc}), where the output signals are the modulation index (M) and the shoot-through duty ratio (D_{sh}) as shown in fig. 7.

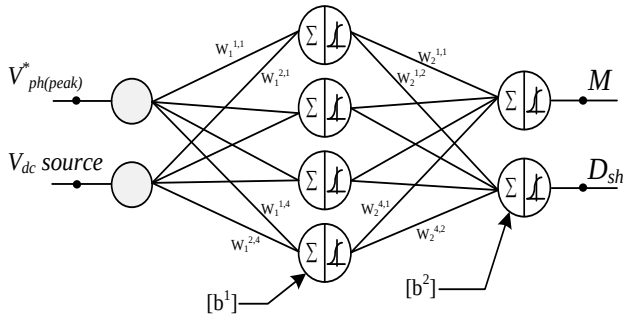

Figure (7): Structure of the M & D_{sh} neural subnet

The second subnet is the timing signal's determination.
$T_A - ON$: $(upper\ and\ lower)$, $T_B - ON(upper\ and\ lower)$,
$T_C - ON(upper\ and\ lower)$. The composite network uses three input neurons, twenty neurons in the hidden layer, and six output neurons. The input signals are the modulation index M, and the shoot-through duty ratio D_{sh} , and the position angle of the reference voltage θ_e^*. The output signals are the six $T_X - ON$ time signals of the inverter devices as shown in fig. 8.

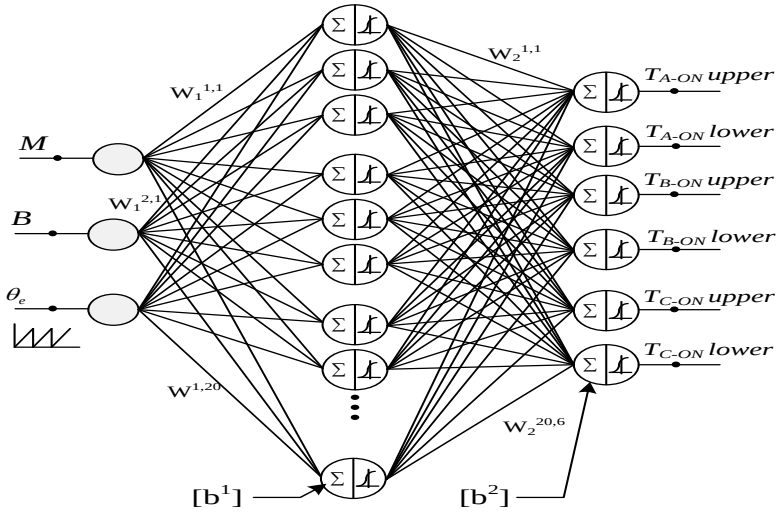

Figure (8): Structure of the T_x-ON time neural subnet

The back-propagation algorithm in the MATLAB Neural Network Toolbox is used for the training. The first subnet takes 300 epochs for training with data of increment in the reference voltage from 0-400 by step of 10V and a constant DC supply of 300V where the second subnet takes 500 epochs for training the output data obtained from the first subnet as an input data to the second subnet with additional third input of position angle of the reference voltage from 0°-360° by increments of 1°. The training data size and the corresponding training time are, thus, reasonable small. It is important to note that, due to learning or interpolation capability, both of the subnets will operate with higher signal resolution. The accuracy performance and output validation of the first subnet can be investigated by swept the reference input $\hat{V}_{ph}^{*}$ from 0-800 and using V_{dc}=200V to obtain voltage gain 0-4, the output signals M and D_{sh} are depicted in Fig. 9 in conjunction with conventional DSP-based MSVPWM.

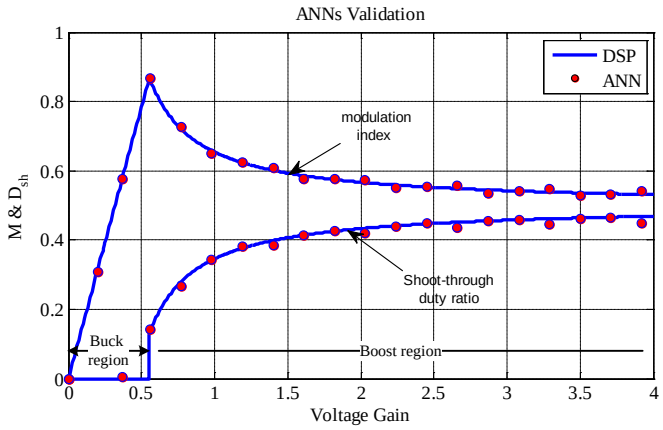

Figure(9). Accuracy performance of the M & D_{sh} neural subnet

In the other hand, the accuracy performance and output validation of the second subnet is shown in fig. 10. Which demonstrates the prediction of $T_X - ON$ time $T_A - ON(upper\ and\ lower)$ for different reference values in the buck and boost operation modes in conjunction with the DSP-based $T_A - ON$ calculation.

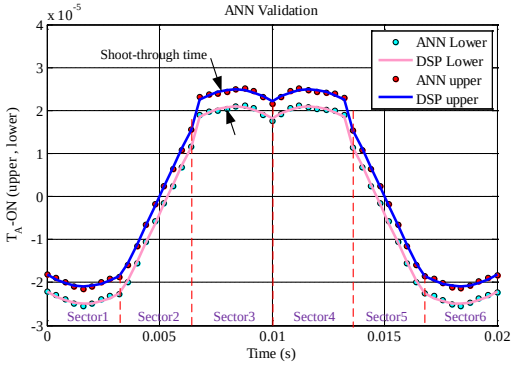

(a)

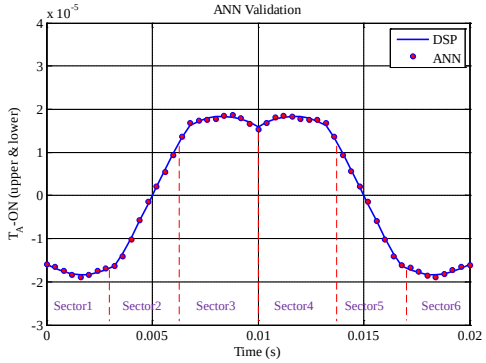

(b)

Figure (10): Accuracy performance of the T_x-ON neural subnet. (a) Boost mode, (b) buck mode.

Simulation results:

In order to realize the features of the proposed method a comparison investigation is done by using the following z-source parameters: Input DC=300V, L_z=250μH, C_z=460 μF, V_{dc}=300V and switching frequency 10kHz. Where, the AC side load is a 5kw three-phase induction motor: 50Hz, 380V, 4-pole. The reference input $\hat{V}_{ph}^{*}$ is varied in steps: 400, 500, 600 and 400. The z-source performance of the capacitor voltage V_c and the DC-link V_{link} are illustrated in fig. 11. The shoot-through duty ratio (D_{sh}), modulation index (M) and voltage stress are shown in fig. 12 for both DSP-based and ANN-based modulators. Result elucidates the salient feature of the proposed method for time saving not only practically but in simulation too. Also, the obtained V_c and V_{link} are soft and less ripple than conventional method, because this method don't need a hold time for computation process as in DSP process. The reduction in voltage stress is about 8% at

voltage gain G=2. The normalized voltage stress across the inverter devices $\hat{V}_{link}/V_{dc}$ of the proposed ANN-based MSVPWM is depicted in fig. 13 in conjunction with the conventional DSP-based method. The values of the voltage stress are obtained from the simulation test for different values of shoot-through duty ratio from 0-0.45. The comparison shows a little reduction in the voltage stress especially for high gain values. A three-dimension surface sketch of the overall system gain versus the variation of shoot-through duty ratio and the modulation index is illustrated in fig. 14. The maximum values of the permitted modulation index for each value of the shoot-through duty ratio are depicted.

Finally, the features of the proposed method can be demonstrated by investigating the performance of both DC-side and AC-side of the z-source inverter. Fig. 15 and 16 shows the performance of the DC-side as response to the same command of the reference voltage (in fig. 11) in cases of 200V and 300V input voltage respectively. The required boosting factor *B*, shoot-through duty ratio D_{sh} and voltage stress, also the desired and obtained DC-link voltages are depicted. The performance shows smooth and fast dynamic response for tracking the input command. By the same conditions of input command and input voltage the performance of the AC-side of the z-source inverter are shown in fig. 17 and 18. The desired peak voltage and the obtained output AC voltage and current, the required system gain and modulation index are depicted.

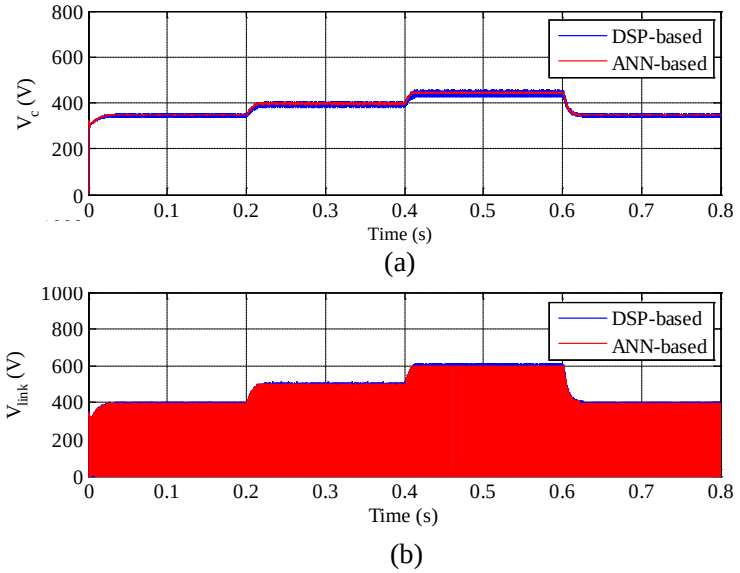

Figure(11). Z-source performance; a) Capacitor voltage, b) DC-link voltage

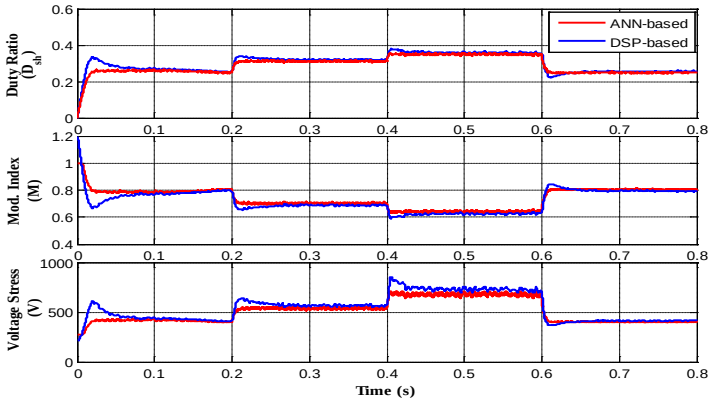

Figure (12) Comparison of D_{sh}, M and voltage stress between ANN and DSP-based modulators

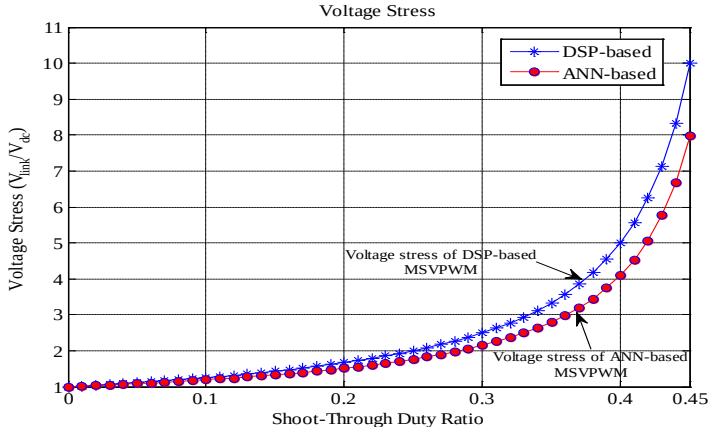

Figure(13). Voltage stress of the ANN and DSP-based modulators

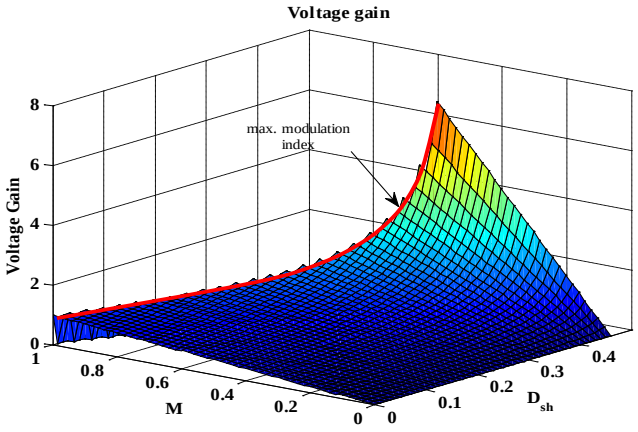

Figure (14): The overall voltage gain of ANN-based MSVPWM

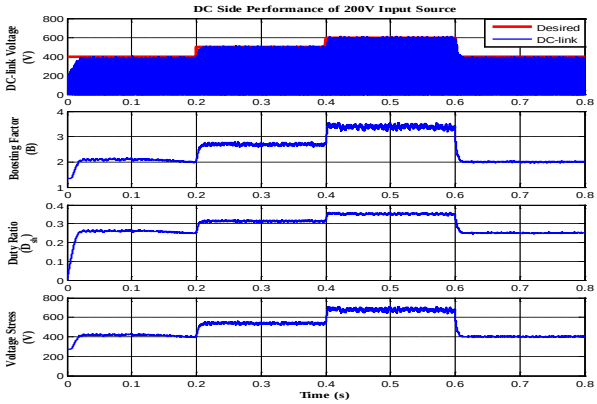

Figure (15): DC-side performance of the z-source inverter in case of 200V input voltage

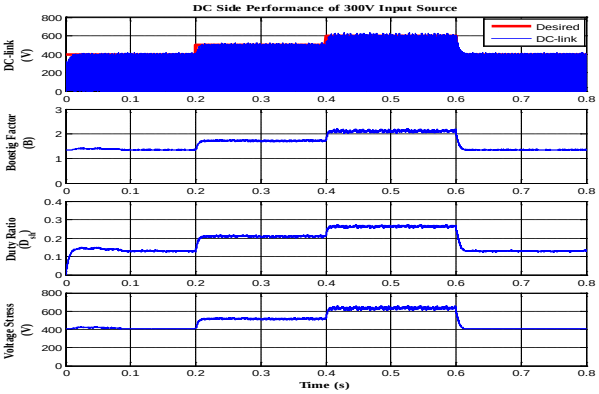

Figure (16): DC-side performance of the z-source inverter in case of 300V input voltage

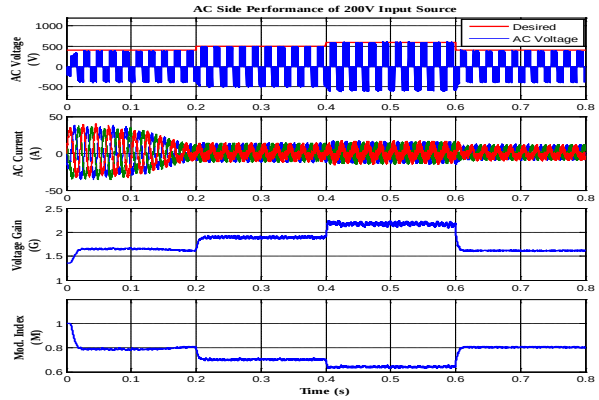

Figure (17): AC-side performance of the z-source inverter in case of 200V input voltage

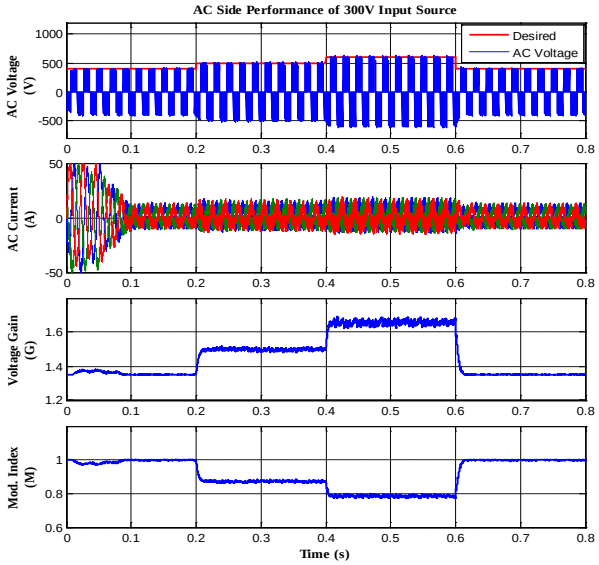

Figure (18): AC-side performance of the z-source inverter in case of 300V input voltage

CONCLUSIONS:

Results elucidate the features of the proposed ANN-based modified SVPWM Z-source inverter. The proposed scheme has been fully evaluated with adjustable speed drive, and gives superior performance over that of conventional DSP-based MSVPWM. The saving of computation delay time process allows the inverter to implement higher switching frequency, which is not possible by conventional DSP-based MSVPWM; this could improve the total harmonic frequency of the load current. Moreover, in case of adjustable speed drive applications the reducing of computation delay time increase the capability of the system to use complex control techniques such as: direct torque or field oriented controllers. In addition, the proposed ANN-based modified SV modulator operates very well in both buck and boost modes and overcomes the discontinuity of modulation index and the shoot-through duty ratio. The voltage stress across the devices in the proposed method is less than of the conventional DSP-based method especially for high gain operation condition.

REFERENCES

[1] F.Z.Peng, "Z-Source Inverter", *IEEE Trans. Industry Applications*, vol. 39, no.2, pp.504-510, March/April, 2003.

[2] Miaosen Shen, " Z-source inverter design, analysis, and its application in fuel cell vehicles", PhD thesis, Michigan State University, 2006.

[3] Peng F. Z., Joseph A., Wang J., Shen M., Chen L., Pan Z. and Huang Y., "*Z-Source inverter for motor drives*", *IEEE Trans. Power Electron.*, Vol. 20, No. 4, pp. 857-863, July 2005.

[4] Rostami H., Khaburi D. A., " *A New Method for Minimizing of Voltage Stress Across Devices in Z-Source Inverter*" , 2nd Power Electronics, Drive systems and Technologies Conference, IEEE, 2011.
[5] Kancheti Karunakar and D.M.Vilathgamuwa, "Dynamic Analysis of Three phase Z-source Boost-Buck Rectifier", 2nd IEEE International Conference on Power and Energy (PECon 08), December 1-3,p.198, 2008, Johor Baharu, Malaysia.
[6] Peng F. Z., Shen M. and Qian Z., "Maximum boost control of the Z-source inverter", *IEEE Trans. Power Electron.*, Vol. 20, No. 4, pp. 833- 838, July 2005.
[7] Shen M., Wang J., Joseph A., Peng F. Z., Tolbert L. M. and Adams D. J., "Maximum constant boost control of the Z-source inverter", *IEEE/IAS*, pp. 142-147, Seattle 2004.
[8] Miaosen Shen, Qingsong Tang, Fang Zheng Peng, "Modeling and Controller Design of the Z-Source Inverter with Inductive Load", IEEE Power Electronics Specialists Conference, 2007, pp: 1804-1809.
[9] Joao O. P. Pinto, Bimal K. Bose, "A Neural-Network-based Space-Vector PWM Controller for Voltage-Fed Inverter Induction Motor Drive", *IEEE TRANSACTIONS ON INDUSTRY APPLICATION*, Vol. 36, No. 6, NOVEMBER/DECEMBER, 2000.
[10] Chun T. W., Tran Q. V., Ahn J. R. and Lai J. S., "AC Output Voltage Control with Minimization of Voltage Stress Across Devices in the Z-Source Inverter using Modified SVPWM", *IEEE APEC*, pp. 1-5, 2008.
[11] Xinping Ding, Zhaoming Qian, Shuitao Yang, Bin Cui, Fangzheng Peng, " A Direct DC-link Boost Voltage PID-like Fuzzy Control Strategy in Z-Source Inverter", IEEE, p.405, 2008.
[12] Vrushali Suresh Neve; P.H. Zope; S.R. Suralkar; "A Literature Survey On Z-Source Inverter", VSRD International Journal of Electrical, Electronics & Communication Engineering, Vol. 2 No. 11 November 2012.
[13] P. C. Loh, D. M. Vilathgamuwa, Y. S. Lai, G. T. Chua, and Y. Li, "Pulse-width modulation of Z-source inverters," *IEEE Transactions on Power Electronics*, vol. 20, pp. 1346-1355, Nov. 2005.